Journal of Power Sources 258 (2014) 420–423

Contents lists available at ScienceDirect

Journal of Power Sources

journal homepage: www.elsevier.com/locate/jpowsour

Short communication

High sodium ion conductivity of glass–ceramic electrolytes with cubic Na_3PS_4

Akitoshi Hayashi*, Kousuke Noi, Naoto Tanibata, Motohiro Nagao, Masahiro Tatsumisago

Department of Applied Chemistry, Graduate School of Engineering, Osaka Prefecture University, 1-1 Gakuencho, Naka-ku, Sakai, Osaka 599-8531, Japan

HIGHLIGHTS

- Na_3PS_4 electrolyte with conductivity of 4.6×10^{-4} S cm^{-1} was prepared.
- High purity of Na_2S contributes to enhancing conductivity of Na_3PS_4 electrolyte.
- All-solid-state sodium batteries ($Na_{15}Sn_4/Na_3PS_4/NaCrO_2$) were fabricated.

ARTICLE INFO

Article history:
Received 8 January 2014
Received in revised form
12 February 2014
Accepted 14 February 2014
Available online 22 February 2014

Keywords:
Solid electrolyte
Sodium battery
All-solid-state battery
Glass–ceramics

ABSTRACT

Sulfide solid electrolytes with cubic Na_3PS_4 phase has relatively high sodium ion conductivity of over 10^{-4} S cm^{-1} at room temperature, and all-solid-state sodium batteries Na–Sn/TiS_2 with the electrolyte operated as a secondary battery at room temperature. To improve battery performance, conductivity enhancement of sulfide electrolytes is important. In this study, we have succeeded in enhancing conductivity by optimizing preparation conditions of Na_3PS_4 glass–ceramic electrolytes. By use of crystalline Na_2S with high purity of 99.1%, cubic Na_3PS_4 crystals were directly precipitated by ball milling process at the composition of $75Na_2S \cdot 25P_2S_5$ (mol%). The glass–ceramic electrolyte prepared by milling for 1.5 h and consecutive heat treatment at 270 °C for 1 h showed the highest conductivity of 4.6×10^{-4} S cm^{-1}, which is twice as high as the conductivity of the cubic Na_3PS_4 glass–ceramic prepared in a previous report. All-solid-state Na–Sn/$NaCrO_2$ cells with the newly prepared electrolyte exhibited charge–discharge cycles at room temperature and kept about 60 mAh per gram of $NaCrO_2$ for 15 cycles.

1. Introduction

Lithium-ion batteries have already been commercially used as rechargeable power sources for mobile devices and vehicle applications. Compared to lithium-ion batteries, sodium-ion batteries are cost-effective because of using natural abundance sodium sources and thus have an advantage for future versatile applications to electric vehicles and backup storages at individual houses and large-scale solar and wind farms [1,2]. In 1970s, transition metal sulfides such as TiS_2 and MoS_2 were studied as positive electrodes for sodium-ion cells [3]. The cells exhibited an excellent cycle performance and the average operating potential is *ca.* 2 V vs. Na^+/Na. Recently, sodium-ion batteries have been intensively studied since hard-carbon was applied as a negative electrode instead of sodium metal [4]. 3 V-class positive electrode materials such as Na_xCoO_2 [5], $NaCrO_2$ [6,7], $NaFeO_2$ [8], and $Na_{2/3}Fe_{1/2}Mn_{1/2}O_2$ [9], and 4 V-class $Na_4Co_3(PO_4)_2P_2O_7$ electrode [10] have been reported. In particular, $NaCrO_2$ exhibits a capacity of *ca.* 120 mAh g^{-1} with satisfied capacity retention in both an organic liquid electrolyte (1 M $NaClO_4$ in PC) [6] and an inorganic ionic liquid (NaFSA-KFSA) [7]. As a negative electrode, several materials of hard carbon [4], Na–Sn alloy [11,12] and $Na_2Ti_3O_7$ [13] have also been found.

Solidification of rechargeable batteries has several merits of high safety, long cycle life and versatile geometries [14–17]. Inorganic solid electrolytes with high sodium ion conductivity are needed to realize all-solid-state sodium batteries. Oxide crystalline electrolytes have been studied and high sodium ion conductivity of over 10^{-3} S cm^{-1} is reported in β-alumina [18] and NASICON-type $Na_3Zr_2Si_2PO_{12}$ [19,20]. These oxide electrolytes need to be sintered at high temperatures of over 1000 °C for reducing grain-boundary resistance. On the other hand, sulfide solid electrolytes have been mainly examined for glassy materials [21,22], and tetragonal Na_3PS_4 is only known to show sodium ion conductivity of

* Corresponding author. Tel./fax: +81 72 2549334.
E-mail address: hayashi@chem.osakafu-u.ac.jp (A. Hayashi).

http://dx.doi.org/10.1016/j.jpowsour.2014.02.054
0378-7753/

10^{-6} S cm^{-1} at 25 °C [23]. Very recently, we have reported a cubic Na_3PS_4 phase was precipitated by crystallization of Na_3PS_4 mother glass and the prepared glass–ceramic electrolyte showed a sodium ion conductivity of 2×10^{-4} S cm^{-1} [24]. Sulfide electrolytes have favorable mechanical properties for fabricating all-solid-state batteries [25]; grain-boundary resistance can be remarkably decreased by only cold press without high temperature sintering, and this is suitable for forming intimate solid–solid interfaces between electrode and electrolyte in all-solid-state batteries. Sulfide electrolytes have lower Young's modulus than oxide electrolytes and this mechanical property contributes to maintain solid–solid contacts during volume changes of electrodes at charge–discharge cycles [25]. In fact, all-solid-state Na–Sn/TiS_2 cells with the Na_3PS_4 glass–ceramic electrolyte prepared by cold press operated as rechargeable sodium batteries at room temperature [24]. The glass–ceramic with cubic Na_3PS_4 phase exhibited the highest conductivity in sulfide electrolytes reported so far. An increase in conductivity of the sulfide glass–ceramics contributes to improving electrochemical performance of all-solid-state sodium cells.

In this study, we have succeeded in an increase in the conductivity of Na_3PS_4 glass–ceramics by twice as the previous report [24]. Crystalline Na_2S with a higher purity was used as a starting material and then preparation conditions for glass–ceramics with cubic Na_3PS_4 were optimized. The prepared glass–ceramic showed the conductivity of 4.6×10^{-4} S cm^{-1} at room temperature and was applied to all-solid-state sodium cells using $NaCrO_2$ active material. This is the first report for all-solid-state sodium cells with a 3 V-class oxide positive electrode.

2. Experimental

Na_3PS_4 glass was prepared by a mechanochemical technique using a planetary ball mill (Fritsch, Pulverisette 7) in the same manner reported [24]. In this study, highly pure Na_2S (99.1 wt%) donated by Nagao Co. was used instead of reagent-grade Na_2S purchased from Sigma–Aldrich Co.; the purity of the latter Na_2S was 95.1 wt%, which was determined using combination of oxidation–reduction titration and neutralization by Nagao Co. The impurities detected are Na_2CO_3, Na_2SO_3 and $Na_2S_2O_3$ and, in particular, the Na_2S reagent (Sigma–Aldrich Co.) includes 4 times larger amount of Na_2SO_3 than the Na_2S reagent (Nagao Co). The starting materials of 75 mol% Na_2S (Nagao Co.) and 25 mol% P_2S_5 (Sigma–Aldrich Co.) were hand-ground and the mixture was then placed into a zirconia (ZrO_2) vessel (internal volume of 45 mL) with 500 ZrO_2 balls (4 mm in diameter). The mechanochemical reaction was performed for 0.5–20 h at a fixed rotation speed of the base disk of 510 rpm. The prepared sample was then heated at 220 or 270 °C for 1–4 h in an electric furnace to prepare glass–ceramics. All processes were performed in a dry Ar atmosphere.

X-ray diffraction (XRD; Rigaku, Ultima IV) measurements of the prepared materials were performed to identify the crystalline phases. Microstructure and size of prepared particles were observed by scanning electron microscope (SEM; JEOL, JSM-6610A). The ionic conductivities of the pelletized samples were measured. Carbon paste was painted to form electrodes on both faces of the pellets. Two stainless-steel disks coupled with Pt wires were attached to the pellets as a current collector. AC impedance measurements were performed for the obtained two-electrode cell in a dry Ar gas atmosphere using an impedance analyzer (Solartron, 1260). Impedance was measured in the frequency range of 0.1 Hz–8 MHz at temperatures from 25 to 100 °C.

An all-solid-state $Na_{15}Sn_4$/$NaCrO_2$ cell with the Na_3PS_4 glass–ceramic electrolyte was fabricated. $NaCrO_2$ active material was synthesized by solid-state reaction in the same manner reported in the literature [6]. A working electrode was prepared by well-mixing of $NaCrO_2$, Na_3PS_4 glass–ceramic electrolyte, and acetylene black (AB) with the weight ratio of 4:6:1. A $Na_{15}Sn_4$–AB composite as a counter electrode was prepared by mechanical milling for the mixture of Na, Sn and AB; the weight ratio of $Na_{15}Sn_4$:AB was 20:3. The formation of a single phase of $Na_{15}Sn_4$ (JCPDS: 071-9879) was confirmed by XRD. The working electrode and the solid electrolyte powders were placed in a 10-mm-diameter polycarbonate tube and pressed together by applying a pressure of 70 MPa. The $Na_{15}Sn_4$–AB composite was then placed on the surface of the solid electrolyte side of the bilayer pellet and a pressure of 360 MPa was applied to the three-layered pellet. The three-layered pellet was sandwiched between two stainless-steel rods as current collectors. Electrochemical tests were conducted at a constant current density of 0.013, 0.064 or 0.13 mA cm^{-2} in the voltage range from 1.2 to 4.0 V at room temperature under an Ar atmosphere using a charge–discharge measurement device (Nagano Co., BTS-2004).

3. Results and discussion

Fig. 1 shows X-ray diffraction (XRD) patterns of Na_3PS_4 samples prepared by mechanical milling for different periods of time. Diffraction peaks attributable to starting materials of Na_2S and P_2S_5 disappear after milling of 1.5 h and the peaks attributable to cubic Na_3PS_4 phase are newly observed. The intensity of the peaks increases with increasing milling periods of time. The XRD pattern of the Na_3PS_4 sample prepared in the previous paper [24] is also shown as comparison. In this study, cubic Na_3PS_4 phase was directly precipitated during milling process for over 0.5 h, while glass was prepared by milling for 20 h in the previous paper. The difference is in the reagent Na_2S used for preparation. The use of reagent Na_2S (99.1 wt%, Nagao Co.) as one of the starting materials results in reducing reaction time to produce glass–ceramic with cubic Na_3PS_4. Direct precipitation of crystalline phases during milling treatment was also reported in the system Li_2S–Al_2S_3 [26]. The use of a high rotation speed (510 rpm) of planetary ball mill gave a direct crystallization of Li_5AlS_4 during ball milling for the mixture Li_2S and Al_2S_3 crystals. Cubic Na_3PS_4 is crystallized via mechanochemical treatment in this study, while impurity components such as Na_2SO_3 in reagent Na_2S used in the previous paper may play an important role on amorphization of electrolytes.

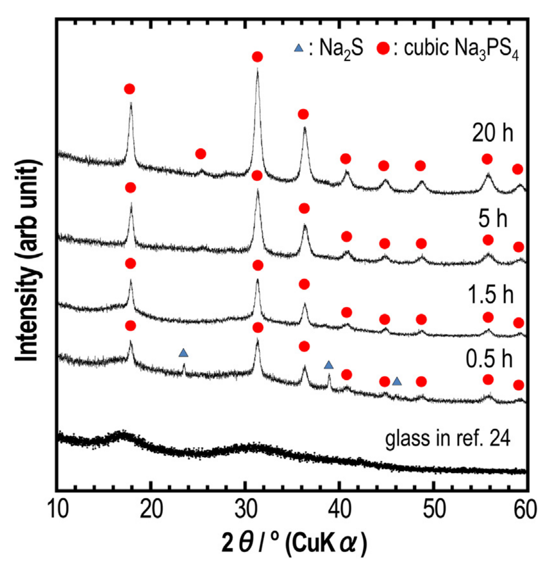

Fig. 1. XRD patterns of Na_3PS_4 samples prepared by mechanical milling for different periods of time. The XRD pattern of the Na_3PS_4 glass prepared by milling for 20 h in the previous paper [24] is also shown as comparison.

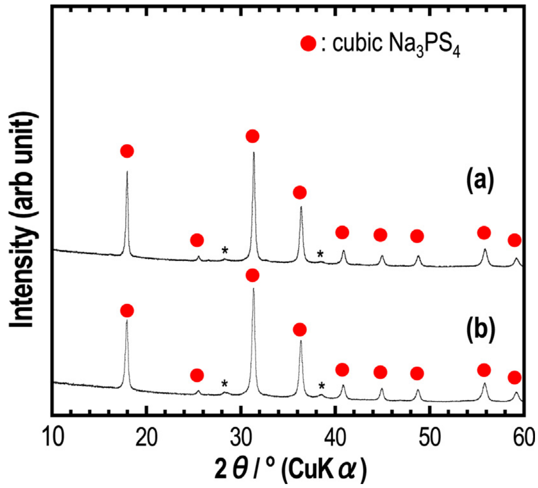

Fig. 2. XRD patterns of Na_3PS_4 glass–ceramics prepared by heat treatment at 270 °C for 2 h for the glass used with Na_2S (Sigma–Aldrich Co.) (a), and the same heat treatment at 270 °C for 2 h for a partially crystallized sample prepared by milling for 1.5 h used with Na_2S (Nagao Co.) (b). The peaks attributable to cubic Na_3PS_4 are denoted with solid circles, and the additional broad peaks with asterisks are the peak only assigned to tetragonal Na_3PS_4.

To improve crystallinity of cubic Na_3PS_4, the milled samples were heat-treated. Fig. 2 shows XRD patterns of Na_3PS_4 glass–ceramics prepared by heat treatment at 270 °C for 2 h for the glass used with Na_2S (Sigma–Aldrich Co.) (a), and the same heat treatment at 270 °C for 2 h for a partially crystallized sample prepared by milling for 1.5 h used with Na_2S (Nagao Co.) (b). The intensity of the peaks attributable to cubic Na_3PS_4 increases with the heat treatment, while the full width of half maximum (FWHM) of the peaks decreases. The FWHM of the glass–ceramic (b) is 0.35°, which is somewhat larger than the FWHM of the glass–ceramic (a), 0.29°. XRD patterns attributable to tetragonal Na_3PS_4 (JCPDS #081-1472) are slightly observed in both the glass–ceramics, but there is no difference in the peak intensity. Fig. 3 shows the temperature dependence of conductivity for the glass–ceramics (a) and (b) denoted in Fig. 2. Conductivity obeys the Arrhenius equation, and activation energy for conduction was calculated. The glass–ceramic (b) shows smaller activation energy of 19 kJ mol^{-1} than the glass–ceramic (a) (27 kJ mol^{-1}). A higher conductivity of 4.6×10^{-4} S cm^{-1} was obtained at room temperature for the glass–ceramic (b), and this value is twice as large as the conductivity of 2.0×10^{-4} S cm^{-1} for the glass–ceramic (a). The glass–ceramics were also prepared by several different milling and heat-treatment conditions. Room temperature conductivity, activation energy for conduction, and FWHM for cubic Na_3PS_4 peaks are summarized in Table 1. FWHM is used as a measure of crystallinity for the glass–ceramics. The FWHM becomes larger with increasing milling periods of time, resulting in decreasing conductivity and increasing activation energy. A higher heat-treatment temperature 270 °C is better for achieving higher conductivity because of higher crystallinity (smaller FWHM); heat treatment time (1 or 2 h) does not largely affect the conductivity and crystallinity. The highest conductivity of 4.6×10^{-4} S cm^{-1} is obtained for the glass–ceramics prepared by milling for 1.5 h and consecutive heat treatment at 270 °C for 1 or 2 h. The use of highly pure reagent Na_2S increases the conductivity of Na_3PS_4 glass–ceramics. The conductivity of glass–ceramics is determined by the following two factors: one is crystallinity of cubic Na_3PS_4 and the other is glass composition partially remained in the glass–ceramics. The improvement of crystallinity of cubic Na_3PS_4 will increase conductivity of glass–ceramics. However, the FWHM of the XRD peaks for cubic Na_3PS_4 was larger in the glass–ceramic prepared from highly pure Na_2S. The grain size of the Na_3PS_4 glass–ceramic is also important, and thus measured by SEM observation. Fig. 4 shows SEM image of the Na_3PS_4 glass–ceramic particles prepared by milling for 1.5 h and consecutive heat treatment at 270 °C for 2 h. Partially aggregate particles with a few micrometer in size are observed. Morphology and size of the secondary particles were almost the same as those of the glass–ceramic particles prepared from the Na_2S reagent (Sigma–Aldrich Co.). Diameter and dispersion of cubic Na_3PS_4 crystallite also affect the conductivity. Therefore, detailed structural analysis by high-resolution TEM observation is further needed for clarifying the effects of cubic Na_3PS_4 component on conductivity of glass–ceramic electrolytes. The glass component also affects the

Table 1
Room temperature conductivities, activation energies for conduction and full width of half maximum (FWHM) of the strongest reflection peak of cubic Na_3PS_4 for glass–ceramics prepared by different mechanical milling (MM) and heat-treatment (HT) conditions.

Preparation condition	σ_{25}/S cm^{-1}	E_a/kJ mol^{-1}	FWHM/°
MM: 20 h → HT: 270 °C, 2 h	1.7×10^{-4}	27	0.40
MM: 5 h → HT: 270 °C, 2 h	3.2×10^{-4}	20	0.37
MM: 1.5 h → HT: 270 °C, 2 h	4.6×10^{-4}	19	0.35
MM: 1.5 h → HT: 270 °C, 1 h	4.6×10^{-4}	19	0.35
MM: 1.5 h → HT: 220 °C, 4 h	3.3×10^{-4}	23	0.38

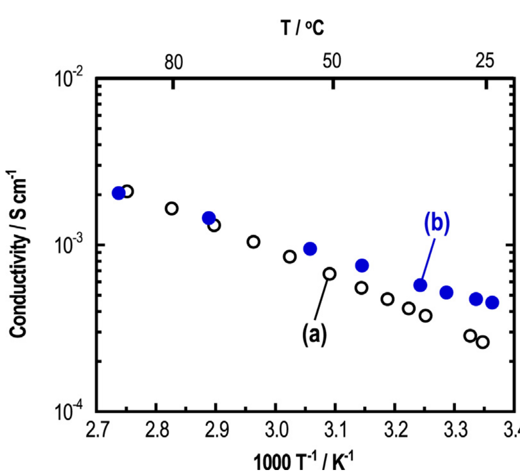

Fig. 3. Temperature dependence of conductivity for the Na_3PS_4 glass–ceramics (a) and (b) denoted in Fig. 2.

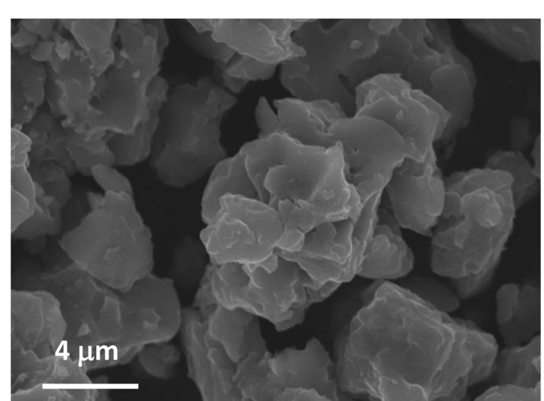

Fig. 4. SEM image for particles of the Na_3PS_4 glass–ceramic (b) denoted in Fig. 2.

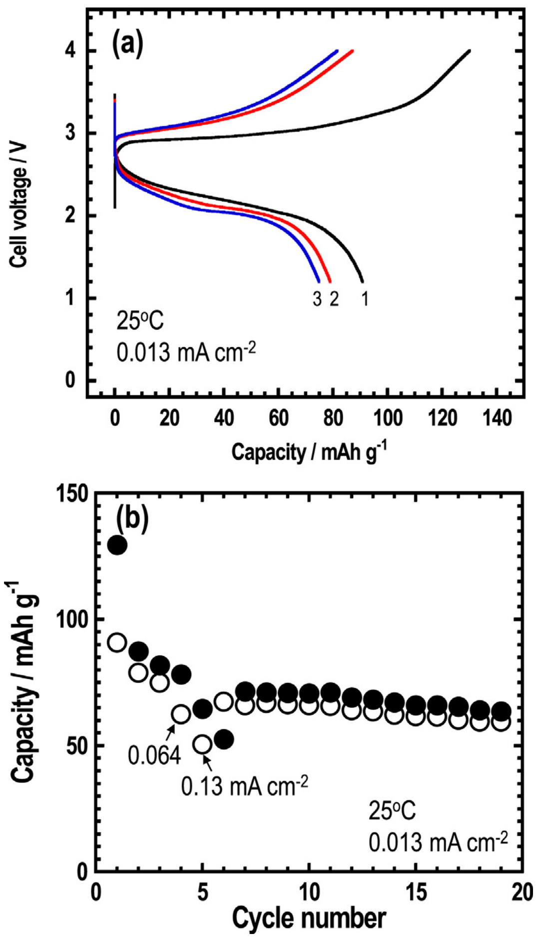

Fig. 5. Initial three charge–discharge curves (a) and cycling performance (b) of an all-solid-state $Na_{15}Sn_4$/cubic-Na_3PS_4 glass–ceramic/$NaCrO_2$ cell. Solid and open marks in figure (b) denote charge and discharge capacities, respectively.

conductivity. The sulfide glass with impurities such as Na_2SO_3 probably has a lower conductivity than the glass with less-impurity because the additional anion species act as a trap for Na^+ cations, resulting in prevention of Na^+ ion conduction.

The glass–ceramic electrolyte with a high conductivity of 4.6×10^{-4} S cm^{-1} was applied to all-solid-state cells. Fig. 5 shows the initial three charge–discharge curves (a) and cycling performance (b) of an all-solid-state $Na_{15}Sn_4$/cubic-Na_3PS_4 glass–ceramic/$NaCrO_2$ cell. The current density was 0.013 mA cm^{-2} except for the 4th cycle (0.064 mA cm^{-2}) and 5th cycle (0.13 mA cm^{-2}). The cell with $NaCrO_2$ operates as a sodium secondary battery at room temperature. The initial charge capacity is *ca.* 130 mAh g^{-1}, which is almost the same as that observed in an electrochemical cell with an organic liquid electrolyte [6]. A large irreversible capacity is observed at the initial cycle. The capacity gradually decreases with initial three cycles and then almost constant capacity of 60 mAh g^{-1} is retained after the 7th cycle. Increase in current density decreases cell capacity at the 4th and 5th cycle. A potential reason for the initial irreversible capacity and capacity fading is the increase of cell resistance. In the all-solid-state lithium cell with $LiCoO_2$ positive electrode and Li_2S–P_2S_5 sulfide electrolyte, a large resistive layer was formed at the interface between the electrode and the electrolyte during the charging process. Surface modification of $LiCoO_2$ particles with oxide thin films such as $LiNbO_3$ [27] or Li_2SiO_3 [28] decreased the interfacial resistance and improved the rate performance of all-solid-state lithium secondary batteries. Detailed structural analyses are important for clarifying stability of the glass–ceramic electrolyte under a high oxidative state in contact with the charged $NaCrO_2$ active material. Surface coating of $NaCrO_2$ with oxide thin films must be effective in developing cell performance and will be examined in the near future.

4. Conclusions

Preparation procedure for glass–ceramic electrolytes with cubic Na_3PS_4 was examined. Cubic Na_3PS_4 was directly obtained via mechanical milling by using highly pure Na_2S (99.1 wt%) reagent as a starting material, which is effective in reducing reaction time to produce glass–ceramics. The glass–ceramic electrolyte prepared by milling for 1.5 h and consecutive heat treatment at 270 °C for 1 h showed the highest conductivity of 4.6×10^{-4} S cm^{-1}. All-solid-state $Na_{15}Sn_4$/$NaCrO_2$ cells with the glass–ceramic electrolyte operated at room temperature and retained about 60 mAh per gram of $NaCrO_2$ for 15 cycles.

Acknowledgments

This research was supported by JST, “Advanced Low Carbon Technology Research and Development Program (ALCA)”.

References

[1] K.B. Hueso, M. Armand, T. Rojo, Energy Environ. Sci. 6 (2013) 734–749.
[2] H. Pan, Y.-S. Hu, L. Chen, Energy Environ. Sci. 6 (2013) 2338–2360.
[3] M.S. Whittingham, Prog. Solid State Chem. 12 (1978) 41–99.
[4] S. Komaba, W. Murata, T. Ishikawa, N. Yabuuchi, T. Ozeki, T. Nakayama, A. Ogata, K. Gotoh, K. Fujiwara, Adv. Funct. Mater. 21 (2011) 3859–3867.
[5] R. Berthelot, D. Carlier, C. Delmas, Nat. Mater. 10 (2011) 74–80.
[6] S. Komaba, C. Takei, T. Nakayama, A. Ogata, N. Yabuuchi, Electrochem. Commun. 12 (2010) 355–358.
[7] C.-Y. Chen, K. Matsumoto, T. Nohira, R. Hagiwara, A. Fukunaga, S. Sakai, K. Nitta, S. Inazawa, J. Power Sources 237 (2013) 52–57.
[8] J. Zhao, L. Zhao, N. Dimov, S. Okada, T. Nishida, J. Electrochem. Soc. 160 (2013) A3077–A3081.
[9] N. Yabuuchi, M. Kajiyama, J. Iwatate, H. Nishikawa, S. Hitomi, R. Okuyama, R. Usui, Y. Yamada, S. Komaba, Nat. Mater. 11 (2012) 512–517.
[10] M. Nose, H. Nakayama, K. Nobuhara, H. Yamaguchi, S. Nakanishi, H. Iba, J. Power Sources 234 (2013) 175–179.
[11] S. Komaba, Y. Matsuura, T. Ishikawa, N. Yabuuchi, W. Murata, S. Kuze, Electrochem. Commun. 21 (2012) 65–68.
[12] T. Yamamoto, T. Nohira, R. Hagiwara, A. Fukunaga, S. Sakai, K. Nitta, S. Inazawa, J. Power Sources 237 (2013) 98–103.
[13] P. Senguttuvan, G. Rousse, V. Seznec, J.M. Tarascon, M.R. Palacin, Chem. Mater. 23 (2011) 4109–4111.
[14] J.-M. Tarascon, M. Armand, Nature 414 (2001) 359–367.
[15] N. Kamaya, K. Homma, Y. Yamakawa, M. Hirayama, R. Kanno, M. Yonemura, T. Kamiyama, Y. Kato, S. Hama, K. Kawamoto, A. Mitsui, Nat. Mater. 10 (2011) 682–686.
[16] K. Takada, Acta Mater. 61 (2013) 759–770.
[17] M. Tatsumisago, M. Nagao, A. Hayashi, J. Asian Ceram. Soc. 1 (2013) 17–25.
[18] A. Hooper, J. Phys. D Appl. Phys. 10 (1977) 1487.
[19] H. Khireddine, P. Fabry, A. Caneiro, B. Bochu, Sens. Actuators B 40 (1997) 223.
[20] W.G. Coors, J.H. Gordon, S.G. Menzer, US Patent US2010/0297537A1, 2010.
[21] M. Ribes, B. Barrau, J.L. Souquet, J. Non-Cryst. Solids 38 & 39 (1980) 271.
[22] W. Yao, S.W. Martin, Solid State Ionics 178 (2008) 1777–1784.
[23] M. Jansen, U. Henseler, J. Solid State Chem. 99 (1992) 110.
[24] A. Hayashi, K. Noi, A. Sakuda, M. Tatsumisago, Nat. Commun. 3 (2012) 856.
[25] A. Sakuda, A. Hayashi, M. Tatsumisago, Sci. Rep. 3 (2013) 2261.
[26] A. Hayashi, T. Fukuda, S. Hama, H. Yamashita, H. Morimoto, T. Minami, M. Tatsumisago, J. Ceram. Soc. Jpn. 112 (2004) S695–S699.
[27] N. Ohta, K. Takada, I. Sakaguchi, L. Zhang, R. Ma, K. Fukuda, M. Osada, T. Sasaki, Electrochem. Commun. 9 (2007) 1486–1490.
[28] A. Sakuda, A. Hayashi, M. Tatsumisago, Chem. Mater. 22 (2010) 949–956.